2011 50th IEEE Conference on Decision and Control and
European Control Conference (CDC-ECC)
Orlando, FL, USA, December 12-15, 2011

Periodic Constraint-Based Control Using Dynamic Wireless Sensor Scheduling

James Weimer, José Araújo, Aitor Hernandez and Karl Henrik Johansson

***Abstract*— Constraint-based control over wireless sensor networks (WSNs) require control strategies that achieve a desired closed-loop system performance while using minimal network resources. In addition to constraints associated with distributed control, WSNs have limitations on bandwidth, energy consumption, and transmission range. This paper introduces and experimentally evaluates a new receding-horizon approach for performing constraint-based control using a WSN. By leveraging the system controllability, the receding-horizon controller is formulated as a mixed-integer programming problem which, at each time step, simultaneously generates a control sequence and sensor selection schedule such that the desired performance is achieved while minimizing the energy required to perform data acquisition and control. For systems containing many sensors, a multi-step state estimator is employed to implement the receding-horizon controller using a conservative abstraction-relaxation approach that simplifies the original mixed-integer programming problem into a convex quadratic programming problem. A wireless process control test bed consisting of 8 coupled water tanks and 16 wireless sensors are used to experimentally evaluate the receding-horizon controller.**

I. Introduction

In recent years, control systems have increasingly been implemented over large-scale networked infrastructures in place of standard wired networks. Using a wireless communication technology to close the control loop provides major advantages in terms of increased flexibility, and reduced installation and maintenance costs. Following this trend, several vendors are introducing devices that communicate over low-power wireless sensor networks (WSNs) for industrial automation and process control. Using these devices, WSNs have been widely analyzed and deployed to extract information from the physical world for the purposes of estimation and detection [1].

When a WSN is used to gather sensor measurements for the purposes of control, network energy usage must be incorporated in the controller design. Over-sampling and network congestion both serve to deplete the lifetime of a WSN containing sensors with a limited battery capacity. Recently, new policies have been introduced which drop the periodicity assumption for sensing and control, such as event-triggered and self-triggered control [2]–[5]. In all these approaches, the control laws are previously designed to guarantee stability of the closed-loop system, and the focus is on how to implement such algorithms taking into account computation and network constraints. Other researchers have addressed network congestion issues using sophisticated networking protocols [6]–[9], however, these approaches assume a known sensing schedule or rate.

Another method of extending the network lifetime is to employ sensor scheduling, where sensor scheduling is the process of identifying which sensors (if any) should report a measurement at each periodic sampling instance. Identifying a sensing schedule has been extensively studied for the purposes of estimation [10], and more recently sensor selection has been introduced for detection [11], [12], as a means of decreasing the network congestion and extending the WSN lifetime; however, these results have not been extended to control applications. A significant obstacle in applying sensor selection for the purposes of control is the requirement that some measure of the closed-loop system performance be maintained (for instance, designing a pump controller and sensor schedule such that the water tank level remains probabilistically bounded). In this paper, we address the issue of simultaneously establishing a control sequence and sensing schedule such that a desired closed-loop performance constraint is satisfied. Specifically, we introduce a new receding-horizon controller that probabilistically bounds the closed-loop system performance while minimizing the number of sensors required to transmit measurements at each time step.

The following section formulates the constrained-control problem considered in this work. Section III introduces a conservative receding-horizon controller based on a finite-horizon solution to the constrained-control problem. Section IV and V presents a multi-step state estimator for the receding-horizon controller and discusses an implementation using a relaxation-abstraction approach, respectively. A process control test bed consisting of 20 sensors is introduced in VI and experimental results are provided in VII. The final section provides discussion and future directions for research.

II. Problem Formulation

In this work we consider the standard time-varying linear stochastic system

$$\begin{aligned} x_{k+1} &= A_k x_k + B_k u_k + w_k \\ y_k &= C_k x_k + v_k \end{aligned} \tag{1}$$

where $x_k \in R^N$ is the system state, u_k is the control input, $y_k \in R^M$ are the sensor measurements, and (x_0, w_k, v_k) are Gaussian, uncorrelated, and white with known mean

The authors are with the ACCESS Linnaeus Center and the Automatic Control Lab, the School of Electrical Engineering, (KTH) Royal Institute of Technology, Sweden. {weimerj,araujo,aitorhh,kallej}@kth.se
This work is supported by the Swedish Energy Agency, the Swedish Governmental Agency for Innovation Systems (VINNOVA), the Swedish Foundation for Strategic Research (SSF) and the Knut and Alice Wallenberg Foundation.

$(\hat{x}_{0|-1}, 0, 0)$ and known covariance $(S_{0|-1}, W, V)$, respectively. A lossy WSN is used to collect sensor measurements at a centralized controller to determine the stabilizing control sequence, $\{u_0, \dots, u_k\}$, which is transmitted over a lossless channel to the plant actuator. The received sensor measurements at time k, r_k, are modeled as

$$r_k = H_k Q_k y_k, \tag{2}$$

where H_k and Q_k represent the binary *network selection matrix* and *sensor selection matrix* at time k, respectively. A selection matrix is a binary matrix having independent rows with exactly one unit entry per row (meaning there is at most one unit entry per column). In (2), the sensor selection matrix identifies which sensors are selected to report their measurements to the fusion center at each time step, where a unit entry in the m^{th} column indicates that sensor m is selected. In the following, we write $q_k = diag(Q_k^T Q_k)$ to be the *sensor selection vector*.[1]

In (2), the network selection matrix, H_k, indicates the subset of the selected sensor measurements that are received by the fusion center after network losses. We model the network losses using a vector of independent Bernoulli random variables, $\lambda_k = [\lambda_k(1), \dots, \lambda_k(M)]^T$, such that

$$P[\lambda_k(m) = 1] = p_m \tag{3}$$

indicates the probability that (if selected) the measurement of sensor m is received by the fusion center and is assumed to be independent of the sensor measurements, y_k. Additionally, we assume that λ_k is i.i.d in time. Without a loss of generality, this work defines the inner product of the network selection matrix as

$$H_k^T H_k = Q_k \Lambda_k Q_k^T, \tag{4}$$

where $\Lambda_k = diag(\lambda_k)$. This property ensures that H_k has a random number of rows (determined by $trace(Q_k \Lambda_k Q_k^T)$), and has the same number of columns as Q_k has rows.

For notational simplicity in the following, I_m is the m-dimensional identity matrix, $e_{m,n}$ represents the m-dimensional binary vector with a single unit entry in the n-th position, $\mathbf{1}_m$ and $\mathbf{0}_m$ are the m-dimensional column vectors of ones and zeros, respectively, and $\mathbf{0}_{m,n}$ denotes the m by n matrix of zeros. We also define

$$\begin{aligned} &\vec{r}_k \triangleq \left[r_0^T, \dots, r_k^T\right]^T && \vec{x}_k \triangleq \left[x_0^T, \dots, x_k^T\right]^T \\ &\vec{w}_k \triangleq \left[w_0^T, \dots, w_k^T\right]^T && \vec{v}_k \triangleq \left[v_0^T, \dots, v_k^T\right]^T \\ &\vec{u}_k \triangleq \left[u_0^T, \dots, u_k^T\right]^T && \vec{q}_k \triangleq \left[q_0^T, \dots, q_k^T\right]^T \\ &\vec{Q}_k \triangleq diag\left(\{Q_0, \dots, Q_k\}\right) && \vec{H}_k \triangleq diag\left(\{H_0, \dots, H_k\}\right) \\ &\vec{C}_k \triangleq diag\left(\{C_0, \dots, C_k\}\right) \end{aligned} \tag{5}$$

where $\vec{u}_k$, $\vec{x}_k$, and $\vec{q}_k$ are the *control sequence*, *concatenated state*, and *sensor selection schedule*, respectively. We note that for any $k' \leq k$ the state, x_k, and sensor selection vector, q_k, can be written as

$$\begin{aligned} x_{k'} &= (e_{k,k'} \otimes I_N)^T \vec{x}_k \\ q_{k'} &= (e_{k,k'} \otimes I_M)^T \vec{q}_k. \end{aligned} \tag{6}$$

where $x \otimes y$ is the Kronecker product of x and y.

We consider a quadratic cost function of the control sequence, $\vec{u}_k$, and concatenated sensor selection vector, $\vec{q}_k$, similar to the LQG cost function [13], written as

$$L(\vec{u}_k, \vec{q}_k) \triangleq \vec{u}_k^T \Omega_k \vec{u}_k + \vec{q}_k^T \Gamma_k \vec{q}_k^T, \tag{7}$$

where $\Omega_k \succeq 0$ is the controller cost, and $\Gamma_k \succeq 0$ is the network cost. The cost function, $L(\vec{u}_k, \vec{q}_k)$, represents a weighted summation of the energy required to perform control and the energy required to gather additional sensor measurements. While the energy cost, $L(\vec{u}_k, \vec{q}_k)$, is similar to the classical LQG controller cost function, it replaces the state error cost with a network energy cost. The network energy cost can be employed to capture the effects of the expected lifetime of each sensor, where sensors with a low battery level would be given a high weight and vice versa.

In this work, we wish to design a control sequence and sensor selection schedule such that the system does not experience an *error*. An error occurs at time k when $f(x_k) \geq 1$, where

$$f(x_k) = ||F_k x_k + g_k||^2. \tag{8}$$

and $F_k \in R^{N \times N}$ and $g_k \in R^N$. We assume that the values of F_k and g_k are independent of the normally distributed state, x_k, such that the distribution of $f(x_k)$ is not chi-squared. As a performance design constraint, the control sequence and sensor selection schedule must ensure that the probability of error conditioned on the received measurements is always bounded,

$$P\left[f(x_k) > 1 | \vec{r}_k\right] \leq \alpha_k \quad \forall k \in \{1, \dots, \infty\}, \tag{9}$$

where $0 \leq \alpha_k \leq 1$ is the *maximum probability of error* at time k. Using a slight abuse of notation, in the following we refer to

We note that the problem detailed in this section is very similar to stochastic or robust model predictive control (MPC) problems [14] [15], where the former considers stochastic plants such as (1) and the latter constrains the state to remain within some range. While it is true that these research topics are closely related to our problem, this work differs because it considers sensor scheduling as part of the controller design. It will be shown in the following sections how incorporating sensor scheduling into the controller design results in dynamic control strategies that are dependent on both the desired closed-loop performance and the cost of using network resources.

III. Controller Design

In this section, we develop a receding-horizon controller for the constrained-control problem described in the previous section. This section is divided into two subsections. The following subsection introduces an off-line finite-horizon

[1] We note that Q_k can be determined from q_k since Q_k is a selection matrix.

controller that generates a conservative control sequence for a finite window of time. The off-line finite-horizon controller is employed in the final subsection to describe the online receding-horizon controller that dynamically identifies the control sequence and sensor selection schedule.

A. Finite-Horizon Control

In this subsection, we introduce a finite-horizon controller for the problem described in Section II, using a model predictive approach. Without a loss of generality, this section assumes the current time is $k = 0$ and a finite *scheduling window* of J time steps. By combining (7) and (9), the finite-horizon control problem is written as a mixed-integer programming problem as,

$$\begin{aligned} \vec{u}_J, \vec{q}_J = \arg\min_{u,q} & L(u, q) \\ s.t. \quad & P\left[f(x_k) \geq 1 | \vec{r}_k\right] \leq \alpha_k, \quad \forall k \in \{1, \ldots, J\} \\ & q \in \{0, 1\}^{MJ}, \end{aligned} \tag{10}$$

where M is the number of sensors and the second constraint ensures the sensor selection schedule is binary. Although it is not explicitly stated, we note that $P\left[f(x_k) \geq 1 | \vec{r}_k\right]$ is a function of the control sequence, $\vec{u}_k$, and sensor selection schedule, $\vec{q}_{k'}$.

Recalling from (8) that $f(x_k)$ is a quadratic function of the state, x_k, evaluating the probability of failure is difficult since the distribution of $f(x_k)$ is characterized by a weighted sum of noncentral chi-squared random variables [16]. Thus, the following lemma presents a conservative approximation conditioned on the received sensor measurements.

Lemma 1: If $m_{k|k'} = E\left[x_k | \vec{r}_{k'}\right]$, $S_{k|k'} = Cov\left[x_k | \vec{r}_{k'}\right]$, and $k' \leq k$, then

$$h(k|k', k') \leq \alpha \Longrightarrow P\left[f(x_k) \geq 1\right] \leq \alpha \tag{11}$$

where

$$h(k|i, j) = ||F_k m_{k|i} - g_k||^2 + Tr\left[F_k^T F_k S_{k|j}\right] \tag{12}$$

Proof: Since $f(x_k)$ is a quadratic function of Gaussian random variables [17], then $h(k|k', k') = E\left[f(x_k) | \vec{r}_{k'}\right]$. By applying Markov's inequality [18], yields (11) ∎

Lemma 1 indicates that the future probability of error is bounded by a non-linear function of the predicted state-estimate. We note that the future state mean, $m_{k|k'}$, is dependent on the received measurements, while the state covariance, $S_{k|k'}$, only depends on whether a measurement is received and not the actual received value. Since the mean is dependent on the unknown future sensor measurements, maintaining the desired performance requires that the control sequence be designed invariant to the received measurements.

For reasons that will become apparent in the following subsection, we also design the finite-horizon controller to be invariant to the most recent sensor measurements, and write the energy-minimizing finite-horizon controller as the following mixed-integer programming problem:

$$\begin{aligned} \vec{u}_J, \vec{q}_J = \arg\min_{u,q} & L(u, q) \\ s.t. \quad & h(k|k-J, k-J) \leq \alpha_k, \quad \forall k \in \{0, \ldots, J-1\} \\ & q \in \{0, 1\}^{MJ}. \end{aligned} \tag{13}$$

The finite-horizon controller in (13) determines a control sequence and sensor selection schedule for a window of J time steps that minimizes a weighted function of the energy required to perform sensing and control. The finite horizon controller uses a model-predictive approach to bound the probability of error by generating a control sequence and sensor schedule that is invariant to the future measurements and the J most recent sensor measurements.

B. Receding-Horizon Control

The finite-horizon controller introduced in the previous subsection schedules the controller sequence for a finite window of time such that the probability of error is bounded. Typically, a receding-horizon controller is implemented by solving the finite horizon controller at each time step, k, and implementing only the first time step of the resulting control sequence [13]. Since the finite-horizon controller in (13) is a constrained minimization problem, the probability of error can only be bounded if the minimization problem is feasible. Thus, to implement a receding-horizon controller that bounds the probability of error requires that successive instances of the minimization problem in (13) be feasible.

To ensure future minimization problems are feasible requires incorporating the future constraints into the current minimization problem. Assuming a scheduling window of J time steps, we write the receding-horizon controller that ensures the next K minimization problems are feasible as

$$\begin{aligned} & \vec{u}_{J+K}, \vec{q}_{J+K} = \arg\min_{u,q} L(u, q) \\ & s.t. \quad h(k|k-J, k-J) \leq \alpha_k, \quad \forall k \in \{1, \ldots, J+K\} \\ & \quad q \in \{0, 1\}^{M(J+K)} \end{aligned} \tag{14}$$

While the constrained minimization problem in (14) ensures that future instances of the finite-horizon control problem are feasible, we observe that the constraint on $h(k|i, j)$ when $i \geq 0$ requires knowledge of the future received observations. Since the future observations are unknown, the remainder of this subsection develops a heuristic approach for the receding-horizon controller in (19) that leverages the system controllability to ensure that future minimization problems are feasible.

Without loss of generality in the following, we assume the current time is $k = 0$ and introduce new notation for the control sequence. We write $u_{k|k'}$ to be the controller input at time k, which is calculated at time k', where $k' \leq k$ and define

$$\hat{u}_{k|k'} \triangleq \left[\begin{array}{cccccc} u_{0|0}^T & \ldots & u_{k'-1|0}^T & u_{k'|k'}^T & \ldots & u_{k|k'}^T \end{array}\right]^T. \tag{15}$$

The definition of $\hat{u}_{k|k'}$ indicates that the control sequence is comprised of two subsequences, the former subsequence is calculated at the current time while the latter subsequence is calculated at some future time k'. We refer to the time when the latter controller sequence is calculated as the *controller transition time*. Additionally, we claim the system in (1) is *mean-controllable* at time k in J time steps if

$$rank \left[\begin{array}{cccc} B_{k+J} & A_{k+J}B_{k+J-1} & \dots & \prod_{i=k}^{k+J} A_i B_k \end{array} \right] = N, \tag{16}$$

where the state estimate of a mean-controllable system can be driven to any value in J time steps.

We note that the state estimate, $m_{k|k'}$, is dependent on the control sequence, $u_{k|k'}$ and by requiring (1) to be mean-controllable in J time steps, we introduce the following lemma.

Lemma 2: If (1) is mean-controllable in J time-steps, then for any state estimate, $m_{J+k|-1}$, there exists a control sequence, $\hat{u}_{J+k|k}$, such that

$$m_{J+k|k} = m_{J+k|-1}. \tag{17}$$

Proof: A direct result of controllability [13]. ■

In words, the above lemma states that if a system is controllable in J time steps, then regardless of how the first k sensor measurements update the state estimate at time k, there exists an initially unknown control sequence of J time steps (which must be determined in the future at time k) such that the state estimate conditioned on the received measurements up to time k equals the initially predicted state estimate at time $k+J$.

Applying lemma 2 to (12), we write for $k' \geq -1$,

$$h(k|k'-J,k') \leq \alpha_k \Longrightarrow h(k|k',k') \leq \alpha_k \quad \exists \vec{u}_{k|k'}, \tag{18}$$

when the system in (1) is mean-controllable in J time steps. Assuming optimality and J step mean-controllability, we write the receding-horizon controller as

$$\begin{aligned} \vec{u}_{J+K}, \vec{q}_{J+K} = & \arg\min_{u,q} L(u,q) \\ & s.t. \;\; h(k|\min(k-J,-1), k-J) \leq \alpha_k, \\ & \qquad \forall k \in \{1,\dots,J+K\} \\ & \qquad q \in \{0,1\}^{M(J+K)} \end{aligned} \tag{19}$$

where the first constraint employs (18) such that for each constraint involving $h(k|i,j)$ when $i \geq 0$, the constraint is replaced with $h(k|-1,j)$, which is invariant to future observations.

Unlike other model-predictive approaches, the proposed receding-horizon approach does not attempt to drive the state to zero and is therefore not asymptotically stable. Rather, the proposed approach allows the controller to design a control sequence that may drive the state away from zero, so long as the predicted state is likely to not result in an error. By requiring that the probability of error be bounded at all times in the horizon, the controller input is constrained such that the resulting state estimate is not likely to result in an error.

When the system in (1) is mean-controllable in one time step, then by choosing $J = 1$ and $K = 1$, the receding-horizon controller guarantees that the next step minimization problem is feasible. However, for systems not mean-controllable in 1 time step the receding horizon-controller is a heuristic since the statement in (18) only claims the existence of a future control sequence to bound a single constraint, not multiple constraints. When the system is not one-step controllable, choosing the finite-horizon scheduling window, J, and the feasibility window, K, becomes a trade off between the complexity required to schedule for longer periods versus the likelihood that future probability of error is bounded.

This section introduced a receding-horizon controller for the constraint-based control problem posed in section II that determines a control sequence and sensor selection schedule that bounds the probability of error over a finite window, J, and is likely to bound the probability of error for times beyond J. The receding-horizon controller employs the finite horizon controller to bound the current probability of error and leverages the system controllability as a heuristic to ensure the probability of error in the future can be bounded.

IV. Estimator Design

The receding-horizon controller in (19) requires estimating the state over multiple time steps where a multi-step recursive solution is known to be a complicated function of the network selection matrix and sensor selection matrix [19], [20]. To avoid this complexity, we recall that the system model in (1) and the measurement model in (2) are linear, such that the concatenated state at time k, $\vec{x}_k$, and the concatenated received measurement at time k', $\vec{r}_{k'}$, can be modeled as

$$\begin{aligned} \vec{x}_k &= \Psi_x(k,0)x_0 + \Psi_u(k)\vec{u}_{k-1} + \Psi_w(k)\vec{w}_{k-1} \\ \vec{r}_{k'} &= \Upsilon_{k'} \left(\mathcal{C}_{k|k'}\vec{x}_k + \vec{v}_k \right) \end{aligned} \tag{20}$$

where $k' \leq k$ and

$$\begin{aligned} \Upsilon_{k'} &\triangleq \vec{H}_{k'}\vec{Q}_{k'} \\ \mathcal{C}_{k|k'} &\triangleq \left[\begin{array}{cc} \vec{C}_{k'} & \mathbf{0}_{Mk,N(k-k')} \end{array} \right] \\ \Psi_x(k) &\triangleq \left[\begin{array}{cccc} I & A_0^T & \dots & \left(\prod_{i=0}^{k-1} A_i \right)^T \end{array} \right]^T \\ \Psi_w(k) &\triangleq \left[\begin{array}{ccc} \Delta_{0,k} & \dots & \Delta_{k-1,k} \end{array} \right] \\ \Psi_u(k) &\triangleq \left[\begin{array}{ccc} \Delta_{0,k}B_0 & \dots & \Delta_{k-1,k}B_{k-1} \end{array} \right] \\ \Delta_{j,k} &\triangleq \left[\begin{array}{cccccc} \dots & 0 & I & A_{j+1}^T & \dots & \left(\prod_{i=j+1}^{k-1} A_i \right)^T \end{array} \right]^T \end{aligned} . \tag{21}$$

The concatenated system model in (20) models the state from time 0 to k and the received sensor measurements from time 0 to k', where $k' \leq k$. Since the concatenated model in (20) is linear and Gaussian, we apply a Kalman filter to estimate the concatenated state, written as

$$\begin{aligned}
\vec{m}_{k|-1} =&\Psi_x(k)\hat{x}_{0|-1} + \Psi_u(k)\vec{u}_{k-1}\\
\vec{S}_{k|-1} =&\Psi_x(k)S_{0|-1}\Psi_x^T(k) + \Psi_w(k)(I_{k-1}\otimes W)\Psi_w^T(k)\\
\Sigma_k =&\Upsilon_k\left(\vec{C}_k\vec{S}_{k|-1}\vec{C}_k^T + (I_k\otimes V)\right)\Upsilon_k^T\\
\vec{m}_{k|k'} =&\vec{m}_{k|-1} + \vec{S}_{k|-1}\mathcal{C}_{k|k'}^T\Upsilon_{k'}^T\Sigma_{k'}^{-1}(r_{k'} - \Upsilon_{k'}\mathcal{C}_{k|k'}\vec{m}_{k|-1})\\
\vec{S}_{k|k'} =&\vec{S}_{k|-1} - \vec{S}_{k|-1}\mathcal{C}_{k|k'}^T\Upsilon_{k'}^T\Sigma_{k'}^{-1}\Upsilon_{k'}\mathcal{C}_{k|k'}\vec{S}_{k|-1},
\end{aligned}\tag{22}$$

where $(\vec{m}_{k|-1}, \vec{S}_{k|-1})$ and $(\vec{m}_{k|k'}, \vec{S}_{k|k'})$ characterize the normally distributed *a priori* and the conditional maximum likelihood estimate of the concatenated sate, $\vec{x}_k$, respectively.

The multi-step state estimator developed in this section uses the model information provided in (1) and (2) coupled with the received measurements to identify the maximum likelihood estimate of the concatenated state, $\vec{x}_k$. The multi-step state estimator sacrifices computational complexity such that the state estimate is a non-recursive function of the sensor selection schedule. The multi-step state estimator introduced in this section will be used in the following section to implement the receding horizon controller in (19).

V. IMPLEMENTATION

The receding-horizon sensor scheduler introduced in (19) requires solving a mixed-integer programming problem [21] and results in a potentially exhaustive search of all possible strategies [22], [23], which is computationally infeasible for problems with a large number of sensors or a large scheduling window. To address these issues, this section formulates a relaxation-abstraction approach that is computationally feasible for identifying the control sequence and sensor selection schedule for systems containing a large number of sensors. The following lemma introduces useful properties for formulating a convex relaxation of the sensor scheduling problem.

Lemma 3: Given a positive definite matrix, Σ, and two selection matrices, H and H_c, where $H^TH + H_c^TH_c = I$, then the following are true

$$\begin{aligned}
&(i)\quad \left(H_c\Sigma^{-1}H_c^T\right)^{-1} \preceq H_c\Sigma H_c^T\\
&(ii)\quad H^T\left(H\Sigma^{-1}H^T\right)^{-1}H = \Sigma - \Sigma H_c^T\left(H_c\Sigma H_c^T\right)^{-1}H_c\Sigma\\
&(iii)\quad H^T\left(H\Sigma^{-1}H^T\right)^{-1}H \succeq H^TH\Sigma + \Sigma H^TH\\
&\qquad\qquad - \Sigma H^TH\Sigma^{-1}H^TH^T\Sigma
\end{aligned}\tag{23}$$

Proof: The details of the proof are omitted due to space constraints. Part (i) and (ii) are a direct consequence of the matrix block inverse [17]. Part (iii) results by applying part (i) to part (ii) and simplifying. ■

By applying the property (iii) in Lemma 3 to the trace term of $h(k|i,j)$ in (18), we observe the performance constraints in (19) can be conservatively relaxed since

$$\hat{h}(k|i,j) \le \alpha_k \Longrightarrow h(k|i,j) \le \alpha_k \tag{24}$$

where

$$\hat{h}(k|i,j) = ||\mathcal{D}_1\vec{u}_k + \mathcal{D}_2||^2 + \vec{q}_j^T\mathcal{D}_3\vec{q}_j + \mathcal{D}_4^T\vec{q}_j + \mathcal{D}_5 \tag{25}$$

with, by defining $x\circ y$ to be the Schur product of x and y,

$$\begin{aligned}
\hat{\Sigma} =&\vec{C}_j\vec{S}_{j|-1}\vec{C}_j^T + (I_j\otimes V)\\
\hat{F} =&F_k(e_{k,k}\otimes I_N)^T\\
\mathcal{D}_1 =&\hat{F}\Psi_u(k)\\
\mathcal{D}_2 =&g_k + \hat{F}\Psi_x(k)m_{0|i}\\
\mathcal{D}_3 =&\left(\hat{\Sigma}^{-1}\mathcal{C}_{k|j}\vec{S}_{k|-1}\hat{F}^T\hat{F}\vec{S}_{k|-1}\mathcal{C}_{k|j}^T\hat{\Sigma}^{-1}\right)\circ P_{1,j}\circ\hat{\Sigma}\\
\mathcal{D}_4 =&-2diag(P_{2,j}\hat{\Sigma}^{-1}\vec{C}_k\vec{S}_{k|-1}\hat{F}^T\hat{F}\vec{S}_{k|-1}\vec{C}_k^T)\\
\mathcal{D}_5 =&Tr\left[\hat{F}^T\hat{F}\vec{S}_{k|-1}\right]
\end{aligned}\tag{26}$$

and $P_{1,k}$ and $P_{2,k}$ such that

$$\begin{aligned}
P_{1,k}(i,j) &= \begin{cases} p_i & \text{if } \ i=j\\ p_ip_j & \text{otherwise}\end{cases}\\
P_{2,k}(i,j) &= \begin{cases} p_i & \text{if } \ i=j\\ 0 & \text{otherwise}\end{cases}
\end{aligned}\tag{27}$$

While the relaxed constraint $\hat{h}(k|i,j)$ is a quadratic function of the control sequence and the sensor selection schedule, the resulting mixed-integer programming problem is known to be NP-hard [24], and results (in the worst case) in an exhaustive search [22], [23]. For applications with many sensors or large scheduling windows, this approach is known to be infeasible. Applying a similar approach as in [19], [21], [25], we relax the binary constraint on the sensor selection schedule and write the relaxed-conservative receding-horizon controller using a quadratic programming problem as

$$\begin{aligned}
\vec{u}_{J+K}, \vec{q}_{J+K} = \arg\min_{u,q}&\ L(u,q)\\
s.t.&\ \ \hat{h}(k|min(k-J,-1), k-J) \le \alpha_k,\\
&\qquad \forall k\in\{1,\ldots,J+K\}\\
&\ \ \mathbf{0}_{M(J+K)} \le q \le \mathbf{1}_{M(J+K)}
\end{aligned}\tag{28}$$

which can be solved using the CVX toolbox [26]. The minimization problem in (28) identifies a control sequence and relaxed sensing schedule, where the relaxed sensing schedule violates the constraints in the original mixed-integer programming problem if $\vec{q}_{K+J}$ is not binary. To identify a binary sensor selection vector, the elements are ranked from largest to smallest and iteratively included in the sensor selection schedule (by setting the corresponding element of $\vec{q}_{K+J}$ to one) until all the constraints in the original non-relaxed minimization problem in (19) are satisfied. Once all the constraints are satisfied, all non-unit elements of $\vec{q}_{K+J}$ are set to zero.

The conservative implementation of the receding-horizon controller discussed in this section uses an abstraction-relaxation approach applied to the receding-horizon controller in (19) to generate the control sequence and sensing schedule. The approach is shown to be conservative and ensures that the original performance constraints are satisfied.

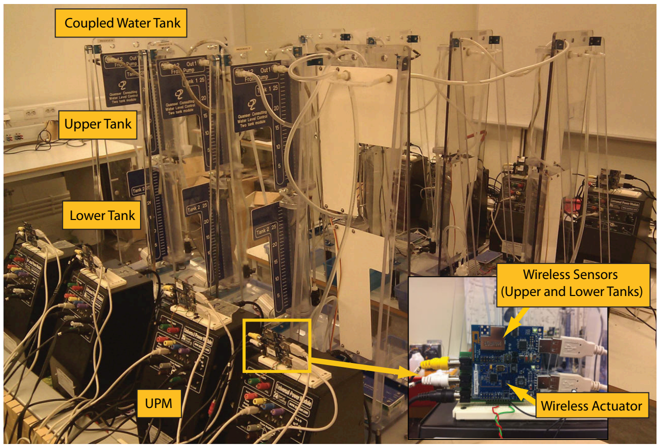

Fig. 1. Setup for the Interconnected Water Tank System and the IEEE 802.15.4 Wireless Sensor and Actuator Network.

The implementable receding-horizon controller formulated in this section is evaluated in section VII using a process control test bed discussed in the following section.

VI. Experimental Setup

To evaluate the performance of the control approach, a test bed representing a scaled version of an industrial setting where a coupled dynamical system is controlled over a wireless network is implemented. The dynamical system consists of eight coupled water tank systems from Quanser [27], where the tanks are collocated with the sensors and actuators and communicate wirelessly with a controller node. Fig. 1 shows the interconnected setup of eight coupled water tank systems and the WSAN.

We now describe the details of the components of our networked control system.

A. Wireless Sensor Nodes

The wireless sensor platform used in this experiment is the Telos wireless node [28]. These nodes are equipped with a 250 kbps 2.4 GHz Chipcon CC2420 IEEE 802.15.4 compliant radio and on-board sensors. Furthermore, each Telos has integrated Analog-to-Digital (ADC) and Digital-to-Analog (DAC) converters that allows us to use them as sensor and actuator nodes. The operating system used is TinyOS [29].

B. Communication Network

The communication protocol used in our networked control setup is the IEEE 802.15.4 [30]. This protocol is the standard for low-power wireless communications and is the base of the wireless industrial protocols WirelessHART and ISA100 [31], [32]. For this setup, we consider the IEEE 802.15.4 protocol in a beacon-enabled mode using a Carrier Sense Multiple Access/Collision Avoidance (CSMA/CA) Medium Access Control (MAC) scheme. The network topology is a star network, where a coordinator node periodically sends a beacon message which synchronizes and configures all the nodes in the network. The communication structure is depicted in Fig. 2, where wireless nodes communicate

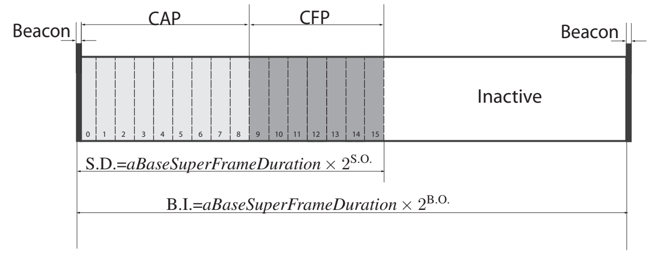

Fig. 2. Communication structure of IEEE 802.15.4. A beacon message is transmitted by the coordinator at the beginning of each superframe in order to synchronize all the nodes in the network. Message transmissions take place during the active period (Contention-Access Period and Collision-Free Period). In the inactive period, the nodes enter a low-power mode in order to save battery.

during an active period, divided by a Contention-Access Period (CAP) and Collision-Free Period (CFP), and enter a low-power mode during an inactive period. More information about the protocol can be found in [30].

C. Interconnected Water Tank System

The Coupled Water Tank system test bed employed in this work consists of eight pumps, a water basin and sixteen tanks of uniform cross sections. This system has similar characteristics to many typical processes used in the chemical industry, e.g. paper mills and ore concentration plants [33]. Furthermore, the control of such a slow process resembles the control of HVAC systems [7].

Fig. 3 depicts the interconnected coupled water tank system. This setup is a variation of the quadruple water tank system [34], for an interconnection of sixteen individual tanks. A pump is responsible for pumping water from the water basin through two sections with different diameters. Through the section with the largest dimensions flows water to the lower tank of the respective water tank system. The smaller section drives water to the upper tank of the adjacent coupled water tank system, which flows to its respective lower tank.

The sensing of the water levels L_i is performed by pressure sensors placed under each tank. The ratio between the sensor measurement and water level is given by $L_i = K_s \cdot V_{out}$, where $K_s = 6.25$ cm/V. The equations describing the dynamics of the interconnected water tank system are nonlinear Thus, in order to apply the proposed techniques, we linearized the dynamics around quiescent points L_{10}, L_{20} for the upper and lower tanks, respectively. This results in the following linear dynamics for each single coupled water tank system:

$$\begin{aligned}\dot{L}_1^j =& -\frac{a_1}{A_1}\sqrt{\frac{g}{2L_{10}}}L_1^j + \frac{\gamma K_p}{A_1}V_p^{j-1} \\ \dot{L}_2^j =& \frac{a_1}{A_2}\sqrt{\frac{g}{2L_{10}}}L_1^j - \frac{a_2}{A_2}\sqrt{\frac{g}{2L_{20}}}L_2^j + \frac{(1-\gamma)K_p}{A_2}V_p^j.\end{aligned} \tag{29}$$

where, coefficient j denotes the $j-th$ coupled water tank system, a_i is the outflow diameter of upper and lower tanks, A_i is the diameter of the upper and lower tanks, g is the

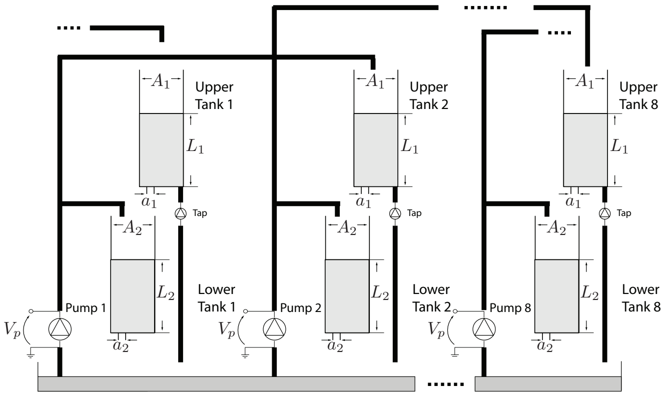

Fig. 3. Interconnected Water Tank System with 8 coupled water tanks [27], each composed by a lower and upper tank.

gravitational acceleration in cm/s^2, V_p is the voltage applied to the pump motor, K_p is the pump motor constant, and L_i is the height of the water in both upper and lower tanks. Moreover, $\gamma = \frac{o_1}{o_1+o_2}$ defines the split of water flow in proportion to the areas of the pump output orifices o_1 and o_2 For this system we have the following parameters: $a_1 = a_2 = 0.178\text{cm}^2$, $A_1 = A_2 = \text{cm}^2$, $K_p = 2.775\text{cm}^3/\text{Vs}$, $g = 9.8\text{m/s}^2$ and $o_1 = 0.635\text{cm}$ and $o_2 = 0.4763\text{cm}$.

Our objective will be to maintain the water level in all the lower tanks L_2 within a pre-defined region by adjusting the motor voltage V_p for all the eight tank systems.

VII. Experimental Results

The experimental test bed described in the previous section is employed to evaluated the performance of the receding-horizon controller. To generate the system model, we assume a sampling time of 1.9 seconds and discretize a continuous-time linear system implementation of (29). In this experiment, we claim an error occurs if any of the lower water tanks' differ by more than ± 5 centimeters of a time-varying reference, X_k, defined as

$$X_k = \begin{cases} 15 & \text{if } \ t \leq 475 \ \text{ sec} \\ 12.5 + 2.5\cos\left(\frac{2\pi}{60}(k-250)\right) & \text{otherwise} \end{cases} \tag{30}$$

The maximum probability of error is $\alpha = 0.10$ and the state dimension equals the number of sensors and tanks, $N = M = 16$. We assign a finite-horizon window of $J = 3$, and a feasibility window of $K = 2$. The controller cost, Ω_k, and the network cost, Γ_k, are

$$\Omega_k = I_{40} \quad \text{and} \quad \Gamma_k = 100 \times I_{80}. \tag{31}$$

Fig. 4 illustrate the tank level measurements versus time. In Fig. 4, the solid lines are the water tank level measurements and the dashed lines represent the ± 5 centimeter envelope around the reference signal. In this experiment, since the state cannot be directly measured, the estimated lower water tank levels conditioned on the received sensor measurements is plotted versus time. Here we observe that the controller is able to maintain the desired performance over the entire experiment. When the reference is static ($t \leq 475$), we observe that the tank water levels vary marginally from the steady state, where the tank levels vary by about one centimeter. When the reference signal is static, the estimated tank levels remain within the required bounds, and vary with the reference signal. The tank levels vary with the reference signal since the foal

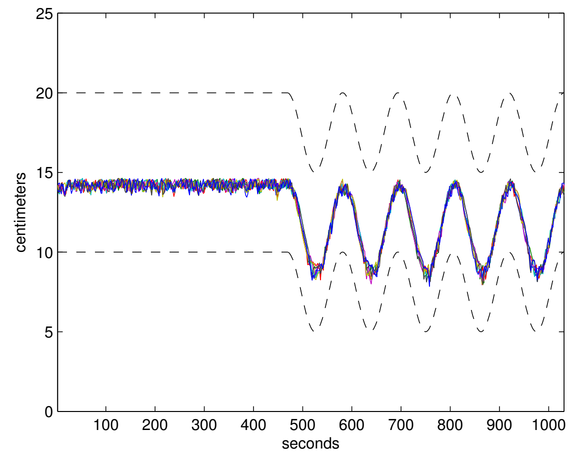

Fig. 4. Lower water tank levels (cm) versus time (s)

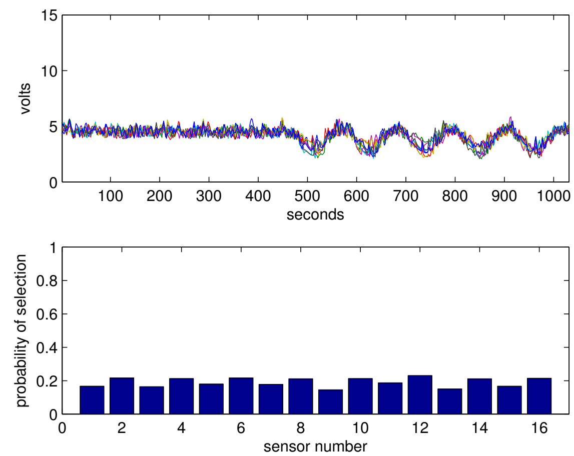

Fig. 5. Control sequence vs. time and sensor probability of selection

The controller input and the sensor rate of selection is selected is shown in Fig. 5, where the top subplot represents the control sequence and the lower subplot illustrates the probability of selecting each sensor. For the control sequence in Fig. 5, we observe that the controller does not reach a steady state solution for a static reference. This is because the control sequence is calculated using the receding-horizon controller which is memoryless with respect to the previously calculated control sequence. However, the control sequence rarely deviates by more than 1 volt from the central value of 5 volts.

The sensor selection subplot in Fig. 5 illustrates that the even sensors (corresponding to the lower tank sensors) are selected on average 22% of the time, which is slightly more often than the upper tank sensor selection of 18%. By applying sensor selection to constraint-based control, the active power associated with sampling a WSN is reduced by a factor of four. Moreover, no single sensor is sensed significantly more than another. These results indicate that for the water tank test bed, a desired bound on the probability of error can be maintained while significantly reducing the number of sensors transmitting measurements.

VIII. Discussion and Future Work

A periodic receding-horizon controller is developed for performing constraint-based control when sensor measurements are collected using a WSN. The receding-horizon controller employs a finite-horizon controller that bounds the probability that a quadratic function of the state exceeds a pre-specified bound, where exceeding the bounds results in an error. The receding-horizon controller is proven to generate a control sequence and sensor selection schedule that ensures the probability of error is bounded for a finite window of time. The optimal control sequence and sensor selection schedule is shown to be the solution to a mixed-integer programming problem, which is solved using a conservative abstraction-relaxation approach for large-scale systems.

Future extensions of this work include a characterization of the stability criteria in terms of the system dynamics and network performance constraints. Another direction of future research is to extend the receding-horizon controller to a distributed approach, since the current formulation assumes a centralized controller. Additionally, the current formulation assumes an independent channel reliability model and does not account for the correlated effects of gathering measurements in a multi-hop network.

References

[1] I. Akyildiz and I. Kasimoglu, "Wireless sensor and actuator networks: research challenges," *Ad hoc networks*, vol. 2, no. 4, pp. 351–367, 2004.

[2] K. Aström and B. Bernhardsson, "Comparison of Riemann and Lebesgue sampling for first order stochastic systems," *Proceedings of the 41st IEEE Conference on Decision and Control*, vol. 2, 2002.

[3] K. Arzén, "A simple event-based PID controller," *Preprints 14th World Congress of IFAC. Beijing, China*, 1999.

[4] P. Tabuada, "Event-triggered real-time scheduling of stabilizing control tasks," *IEEE Transactions on Automatic Control*, vol. 52(9), pp. 1680–1685, 2007.

[5] A. Anta and P. Tabuada, "To sample or not to sample: Self-triggered control for nonlinear systems," *IEEE Transactions on Automatic Control*, vol. 55, no. 9, pp. 2030–2042, 2010.

[6] P. Antsaklis and J. Baillieul, "Technology of networked control systems," *Proceedings of the IEEE*, vol. 95, no. 1, Jan. 2007.

[7] T. Arampatzis, J. Lygeros, and S. Manesis, "A survey of applications of wireless sensors and wireless sensor networks," in *Proceedings of the IEEE International Symposium on Intelligent Control, Mediterrean Conference on Control and Automation*, 2005, pp. 719–724.

[8] M. Cantoni, E. Weyer, Y. Li, S. Ooi, I. Mareels, and M. Ryan, "Control of large-scale irrigation networks," *Proceedings of the IEEE*, vol. 95, no. 1, pp. 75–91, 2007.

[9] P. Park, C. Fischione, and K. H. Johansson, "Adaptive IEEE 802.15.4 protocol for energy efficient, reliable and timely communications," in *ACM/IEEE International Conference on Information Processing in Sensor Networks*, 2010.

[10] H. Rowaihy, S. Eswaran, M. Johnson, D. Verma, A. Bar-noy, and T. Brown, "A survey of sensor selection schemes in wireless sensor networks," in *In SPIE Defense and Security Symposium Conference on Unattended Ground, Sea, and Air Sensor Technologies and Applications IX*, 2007.

[11] D. Bajovic, B. Sinopoli, and J. Xavier, "Randomized sensor selection in sequential hypothesis testing." pp. 2342 – 2354, 2011.

[12] V. Srivastava, K. Plarre, and F. Bullo, "Randomized sensor selection in sequential hypothesis testing," Sept. 2009, available at http://arxiv.org/abs/0909.1801.

[13] J.Bay, *Fundamentals of Linear State Space Systems*. McGraw-Hill, 1998.

[14] M. Bichi, G. Ripaccioli, S. Di Cairano, D. Bernardini, A. Bemporad, and I. Kolmanovsky, "Stochastic model predictive control with driver behavior learning for improved powertrain control," in *Proc. 49th IEEE Conf. on Decision and Control, Atlanta, GA, USA*, Dec 2010, p. 60776082.

[15] E. C. Kerrigan and J. M. Maciejowski, "Robust feasibility in model predictive control: Necessary and sufficient conditions," 2001.

[16] L. L. Scharf, *Statistical Signal Processing, Detection, Estimation, and Time Series Analysis*. Addison-Welsley Publishing Company Inc., Reading, Massachusetts, 1991.

[17] R. Horn and C. Johnson, *Topics in Matrix Analysis*. Cambridge University Press, 1991.

[18] T. M. Cover and J. A. Thomas, *Elements of information theory*. New York, NY, USA: Wiley-Interscience, 1991.

[19] R. A. Y. Mo, L. Shi and B. Sinopoli, "Network Lifetime Maximization via Sensor Selection," in *Proceedings of the Seventh Asian Control Conference, Hong Kong.*, Aug. 2009.

[20] B. Zhu, B. Sinopoli, K. Poola, and S. S. Sastry, "Estimation in wireless sensor network," in *Proceedings of the 26th American Control Conference*, July 2007. [Online]. Available: http://www.truststc.org/pubs/242.html

[21] S. Joshi and S. Boyd, "Sensor selection via convex optimization," *Signal Processing, IEEE Transactions on*, vol. 57, no. 2, pp. 451–462, Feb. 2009.

[22] K. G. Murty, *Linear Complementarity, Linear and Nonlinear Programming*. AHelderman-Verlag, 1988.

[23] A. H. Land and A. G. Doig, "An automatic method of solving discrete programming problems," *Econometrica*, vol. 28, no. 3, pp. 497–520, 1960. [Online]. Available: http://jmvidal.cse.sc.edu/library/land60a.pdf

[24] R. M. Karp, "Reducibility among combinatorial problems," in *Complexity of Computer Computations*, R. E. Miller and J. W. Thatcher, Eds. Plenum Press, 1972, pp. 85–103.

[25] J. Weimer, B. Sinopoli, and B. Krogh, "A relaxation approach to dynamic sensor selection in large-scale wireless networks," *Distributed Computing Systems Workshops, 2008. ICDCS '08. 28th International Conference on*, pp. 501–506, June 2008.

[26] M. Grant and S. Boyd, "Cvx: Matlab software for disciplined convex programming [web page and software]," October 2007. [Online]. Available: http://www.stanford.edu/ boyd/cvx

[27] *Coupled Water Tanks*, Quanser. [Online]. Available: http://www.quanser.com/

[28] J. Polastre, R. Szewczyk, and D. Culler, "Telos: enabling ultra-low power wireless research," *Information Processing in Sensor Networks 2005. Fourth International Symposium on*, Apr. 2005.

[29] D. Gay, P. Levis, and D. Culler, "Software design patterns for tinyos," *SIGPLAN Not.*, vol. 40, no. 7, pp. 40–49, 2005.

[30] *IEEE 802.15.4 standard: Wireless Medium Access Control (MAC) and Physical Layer (PHY) Specifications for Low-Rate Wireless Personal Area Networks (WPANs)*, IEEE, 2006. [Online]. Available: http://www.ieee802.org/15/pub/TG4.html

[31] J. Song, S. Han, A. Mok, D. Chen, M. Lucas, M. Nixon, and W. Pratt, "Wirelesshart: Applying wireless technology in real-time industrial process control," *IEEE Real-Time and Embedded Technology and Applications Symposium*, vol. 0, pp. 377–386, 2008.

[32] A. Willig, "Recent and emerging topics in wireless industrial communications: A selection," *IEEE Transactions on Industrial Informatics*, vol. 4, no. 2, pp. 102 –124, May 2008.

[33] *Socrades*, 6th Framework Programme - European Union. [Online]. Available: http://www.socrades.eu/

[34] K. H. Johansson, "The quadruple-tank process—a multivariable laboratory process with an adjustable zero," *IEEE Transactions on Control Systems Technology*, May 2000.